Research Journal of Engineering Sciences ISSN 2278 – 9472
Vol. **7(11),** 30-39, December **(2018)** *Res. J. Engineering Sci.*

Simulation of the magnetic field in electric machines by the finite element method under FEMM 4.2: case of a definition of short-circuit defect between spiers

Sibiri Wourè-Nadiri BAYOR*, Mawugno Koffi KODJO, Akim Adekunlé SALAMI and Komla A. KPOGLI
Departement of Electrical Engineering, Ecole Nationale Supérieure d'Ingénieurs (ENSI), Université de LOME, TOGO
bayores1@yahoo.fr

Available online at: www.isca.in, www.isca.me
Received 28th August 2018, revised 16th November 2018, accepted 26th December 2018

Abstract

Electrical machines are the main production tools in almost all industrial installations. The major challenges to be overcome for a good continuity of operation of industrial production consist in a thorough knowledge of these machines. Two fundamental problems to be solved by researchers and engineers are the analysis of the characteristics of an existing system and to design another type that will meet a specific need for the improvement of the condition of the machines used in the industrial process. To study any physical system one needs to do a modeling. This will allow engineers to simulate the behavior of the latter who would be exposed to various demands and to deduce the mechanisms that govern its operation. Three methods are often used during this modeling: i. analytical method, ii. semi-numerical method, iii. numerical method: Numerical methods consume a lot of time for calculation. They are based on a computer calculation mode that discretizes the models into elements of rectangular shapes with a Taylor approximation (Finite Difference Method). On the other hand triangular shapes are used with integral formulation or minimization related to stored energy (Finite Element Method). In this article we chose the Finite Element method to design models of electrical machines dedicated to the diagnosis, that is to say healthy operating models and also operating models in the presence of defects. Indeed, it is the short-circuit faults between turns in the asynchronous machines that are taken as an example.

Keywords: Electrical machines, finite elements, mesh, model, defects, magnetic, analysis.

Introduction

The diagnosis of electrical machines has been strongly developed in the industrial world thanks to the desire to obtain a production line that is increasingly efficient and indispensable for certain applications. Production lines must be equipped with effective protection systems because any failure can cause both material and physical damage.

It is to avoid these problems that research has been conducted for decades to develop diagnostic methods such as electromagnetic monitoring. The main purpose of these is to warn factory workers of a possible failure that may occur at a particular point in an industrial process.

Therefore, it is essential to have reliable models of machines to transcribe their behavior.

Analytical methods based on the resolution of local electromagnetic equations called "Maxwell equations" are simple and inexpensive in implementation. These methods become ineffective when one has to take into account the factors inherent to electrical machines such as: the complexity of the geometries, the non-linearity of the magnetic materials and the movement of the rotor with respect to the stator. For semi-numerical methods they take a little more time but only partially answer the shortcomings of the analytical ones, they do not solve the problem related to the non-linearity of the flow all along a flow tube. Numerical methods take considerable computation time but the results obtained are more accurate than the first two[1,2].

The development of computing has provided an adequate tool in solving complex problems. In fact, the increased performances of the computers, both in terms of the evaluation frequencies and the quasi-exponential increase in memory and storage sizes, allow the use of increasingly sophisticated digital models, which translate the taking into consideration a growing number of phenomena governing the operation of electrical machines.

Our goal is to present models of electrical machines where we analyze the magnetic parameters using the finite element method. We present these models by considering some defects that may occur, so magnetic parameter analyzes will be used to diagnose these malfunctions[3].

Finite Element Method[4-6]

In this section will be presented the mathematical equations that describe the phenomena of the electromagnetic field within electrical machines.

Formulations of Equations in Electromagnetism: The local equations of electromagnetism, called Maxwell's equations, describe the local behavior in time and space of electrical and magnetic quantities and their mutual interactions. The following four equations present the most general form of Maxwell's equations:

Maxwell-Faraday equation is given by the relation (1)

$$rot\vec{E} = -\frac{\partial \vec{B}}{dt} \quad (1)$$

Equation of Maxwell-Ampere is given by the relation (2)

$$rot\vec{H} = \vec{J} + \frac{\partial \vec{D}}{dt} \quad (2)$$

Magnetic flux conservation equation is given by the relation (3)

$$div\vec{B} = 0 \quad (3)$$

Maxwell-Gauss equation is given by the relation (4)

$$div\vec{D} = \rho \quad (4)$$

where: $\vec{E}$ (V.m-1) : electric field; $\vec{B}$ (T): magnetic induction; $\vec{H}$ (A.m^{-1}): magnetic field; $\vec{D}$ (C.m^{-2}): electric induction; $\vec{J}$ (C.m^{-2}) : current density; ρ (C.m^{-3}) : volume load; $\frac{\partial \vec{D}}{dt}$: (A.m^{-2}) displacement current density.

The resolution of these equations cannot take place without the constitutive relations of the medium. The relations of the medium are written for the magnetic materials by the relation (5):

$$\vec{B} = \mu * \vec{H} + \vec{B}_r \quad (5)$$

With

$$\mu = \mu_0 * \mu_r \quad (6)$$

where: $\vec{B}_r$ (T) Remanent magnetic induction (case of permanent magnets); μ_0 (H.m^{-1}) Magnetic permeability of the vacuum; μ_r Relative magnetic permeability of the medium; μ (H.m^{-1}) Absolute magnetic permeability.

The relations of the medium are written for the dielectric materials by the relation (7)

$$\vec{D} = \varepsilon \vec{E} \quad (7)$$

With

$$\varepsilon = \varepsilon_0 * \varepsilon_r \quad (8)$$

Where: ε_0 (F.m^{-1}) Permittivity of the vacuum; ε_r Relative electrical permittivity of the medium; ε (F.m^{-1}) Absolute electrical permittivity.

The relation of the Ohm's law is written by the relation (9)

$$\vec{J} = \vec{J}_s + \sigma \vec{E} \quad (9)$$

Where: σ (S.m^{-1}) Electrical conductivity; $\vec{J}_s$ (A.m^{-2}) Density of current from the supply windings.

Previous relationships are given in the most general case: i. in a ferromagnetic material without remanent induction, the term $\vec{B}_r$ of equation (5) becomes null, ii. in the case of permanent magnets, the remanent induction $\vec{B}_r$ is expressed as a function of the magnetization vector $\vec{M}$ according to the equation (10):

$$\vec{B}_r = \mu_0 * \vec{M} \quad (10)$$

Continuity equation: This equation is obtained by the combination of equations (2) and (4) which reflects the conservation of electric charge given by:

$$div\vec{J} + \frac{\partial \rho}{dt} = 0 \quad (11)$$

Formulation of the Electromagnetic Problem

For the frequencies used in electrotechnics, the displacement currents $\frac{\partial \vec{D}}{dt}$ are negligible compared to the conduction currents, which results in $\frac{\partial \vec{D}}{dt} \ll \vec{J}$, the equation (2) is written then:

$$rot\vec{H} = \vec{J} \quad (12)$$

From equation (3) it is possible to introduce a magnetic vector potential $\vec{A}$ such that:

$$\vec{B} = rot\vec{A} \quad (13)$$

According to Helmoltz's theorem, a vector can only be defined if its rotation and divergence are simultaneously given. In this case, the relation (13) is not enough to define the vector $\vec{A}$, we must also define its divergence to guarantee the uniqueness of the solution. In this case, we will use the Coulomb gauge, that is:

$$div\vec{A} = 0 \quad (14)$$

The substitution of (13) in (1) gives us:

$$rot\left(\vec{E} + \frac{\partial \vec{A}}{dt}\right) = 0 \quad (15)$$

The relation (15) implies that there exists a scalar potential *V* such that:

$$\vec{E} + \frac{\partial \vec{A}}{dt} = -g\overrightarrow{rad}V \quad (16)$$

from where:

$$\vec{E} = -\frac{\partial \vec{A}}{dt} - g\overrightarrow{rad}V \quad (17)$$

The substitution of $\vec{E}$ by its expression (17) in equation (7) gives us:

$$\vec{J} = \vec{J}_s - \sigma\left(\frac{\partial \vec{A}}{dt} + g\overrightarrow{rad}V\right) \quad (18)$$

From (5), (12), (13) and (18), the equation governing magnetic phenomena is as follows:

$$rot\left(\frac{1}{\mu}\vec{\nabla}\times\vec{A}\right) = \vec{J}_s - \sigma\frac{\partial \vec{A}}{dt} - \sigma g\overrightarrow{rad}V + rot\left(\frac{1}{\mu}\vec{B}_r\right) \quad (19)$$

In radial flow electric machines (which we are interested in), the arrangement of the conductors in the longitudinal direction favors the establishment of the magnetic field in the transverse planes. The distribution of the field is supposed to be invariant along the longitudinal direction.

In our case, the invariance along the Oz axis, perpendicular to the Oxy plane, results in relations (20) and (21):

$$\vec{A} = A(x, y, t)\vec{e}_z \quad (20)$$

$$\vec{J} = J(x, y, t)\vec{e}_z \quad (21)$$

As a result, equation (19) is written in the form of relation (22):

$$\frac{\partial}{\partial x}\left(\frac{1}{\mu}\frac{\partial A}{\partial x}\right) + \frac{\partial}{\partial y}\left(\frac{1}{\mu}\frac{\partial A}{\partial y}\right) = J_s - \sigma\frac{\partial A}{dt} + \left[\frac{\partial}{\partial x}\left(\frac{1}{\mu}(B_r)_y\right) - \frac{\partial}{\partial y}\left(\frac{1}{\mu}(B_r)_x\right)\right] \quad (22)$$

Boundary conditions: Generally, there are four types of boundary conditions:

$$A = g_0 \quad (23)$$

Dirichlet condition given by the relation (23):

Where: *A*: Unknown function of the problem; g_0: A constant

We speak of homogeneous Dirichlet condition when $A = 0$ along the boundary of the domain.

Neumann condition given by the relation (24):

$$\frac{\partial \vec{A}}{\partial \vec{n}} = g_0 \quad (24)$$

Usually, one speaks of homogeneous Neumann on the planes of symmetry, when $\frac{\partial \vec{A}}{\partial \vec{n}} = 0$ is defined along the border of the domain.

Robin's mixed condition given by the relationship (25). It is the combination of both types of boundary conditions. It is expressed by:

$$aA + b\frac{\partial \vec{A}}{\partial \vec{n}} = g \quad (25)$$

where: a and b: constants defined on the field of study; g: the value of the unknown on the border.

Condition of periodicity and anti-periodicity given by the relation (26). They are also called cyclic and anti-cyclic:

$$A_\Gamma = KA_\Gamma + d_\Gamma \quad (26)$$

Where: A: Unknown function; dΓ: Spatial period (following the contour Γ).

K = 1: Cyclic.
K = - 1: Anti-cyclic.

Transmission Conditions: An electromagnetic field crossing two different continuous media undergoes a discontinuity and is no longer differentiable. In order to solve the Maxwell equations in an entire domain containing sub domains with different material properties, it is therefore necessary to consider the transmission (or interface) conditions, which are as follows:

Conservation of the tangential component of the electric field $\vec{E}$ by the relation (27):

$$\vec{n} \wedge \left(\vec{E}_1 - \vec{E}_2\right) = 0 \quad (27)$$

Conservation of the normal component of magnetic induction $\vec{B}$ given by relation (28):

$$\vec{n} \cdot \left(\vec{B}_1 - \vec{B}_2\right) = 0 \quad (28)$$

Discontinuity of the tangential part of the magnetic field $\vec{H}$, if the surface currents ($\vec{K}_s$) exist, is represented by the equation (29):

$$\vec{n} \wedge \left(\vec{H}_1 - \vec{H}_2\right) = \vec{K}_s \quad (29)$$

Discontinuity of the normal component of the electrical induction $\vec{D}$, if the surface charges ρs exist by the relation (30):

$$\vec{n} \cdot \left(\vec{D}_1 - \vec{D}_2\right) = \rho_s \quad (30)$$

Where: $\vec{n}$ The normal vector at the interface. $\vec{K}_s$ and ρ_s are respectively the current density and the charge density, carried by the separation surface.

Discretization and Approximation

The fundamental idea of the finite element method is to subdivide the region to be studied into small interconnected subregions called finite elements thus constituting a mesh. The unknown functions are approximated in each finite element by a particular function called form function which is continuous and defined on each element alone.

The unknown A in each element e is expressed by a linear combination of the A_i^e values at the nodes as follows:

$$A^e = \sum_{i=1}^{3} \alpha_i^e A_i^e \quad (31)$$

The α_i^e's are the weighting functions that must check the relationship (32):

$$\alpha_i^e(x_j, y_j) = \begin{cases} 0 \; si & i = j \\ 1 \; si & i \neq j \end{cases} \quad (32)$$

In the case of the triangular element (Figure-1), the weighting functions are defined as follows:

$$\alpha_1 = \frac{1}{2\Delta}\left[(x_2.y_3 - x_3 y_2) + (y_2 - y_3).x + (x_3 - x_2).y\right] \quad (33)$$

$$\alpha_2 = \frac{1}{2\Delta}\left[(x_3.y_1 - x_1 y_3) + (y_3 - y_1).x + (x_1 - x_3).y\right] \quad (34)$$

$$\alpha_3 = \frac{1}{2\Delta}\left[(x_1.y_2 - x_2 y_1) + (y_1 - y_2).x + (x_2 - x_1).y\right] \quad (35)$$

where: Δ is the area of the element expressed by the relation (36):

$$2\Delta = \begin{vmatrix} 1 & x_1 & y_1 \\ 1 & x_2 & y_2 \\ 1 & x_3 & y_3 \end{vmatrix} = (x_2.y_3 - y_2.x_3) + (x_1.y_3 - y_1.x_3) + (x_1.y_2 - y_1.x_2) \quad (36)$$

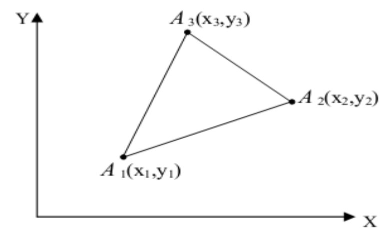

Figure-1: Triangular element.

Integral Formulation: The weighted residuals or integral formulation method leads to the same mathematical developments as the minimization of stored energy. It consists in searching on the field of study the functions A (x, y) which cancel the integral form of the relation (37):

$$\int_{\Omega} \Psi.R(A)d\Omega = 0 \quad (37)$$

With R(A) the residue of the approximation defined by the relation (38):

$$R(A) = L(A) - F_V \quad (38)$$

where: F_V : function defined on the field of study Ω with

$$L(A) = \frac{\partial}{\partial x}\left(\frac{1}{\mu}\frac{\partial A}{\partial x}\right) + \frac{\partial}{\partial y}\left(\frac{1}{\mu}\frac{\partial A}{\partial y}\right) + J_s - \sigma\frac{\partial A}{\partial t} + \left[\frac{\partial}{\partial x}\left(\frac{1}{\mu}(B_r)_y\right) - \frac{\partial}{\partial y}\left(\frac{1}{\mu}(B_r)_x\right)\right] \quad (39)$$

The substitution of (39) in (37), allows us to obtain (40):

$$\iint_{\Omega} \Psi \cdot \left(\frac{\partial}{\partial x}\left(\frac{1}{\mu}\frac{\partial A}{\partial x}\right) + \frac{\partial}{\partial y}\left(\frac{1}{\mu}\frac{\partial A}{\partial y}\right) + J_s - \sigma\frac{\partial A}{\partial t}\right) d\Omega + \iint_{\Omega} \Psi \cdot \left(\left[\frac{\partial}{\partial x}\left(\frac{1}{\mu}(B_r)_y\right) - \frac{\partial}{\partial y}\left(\frac{1}{\mu}(B_r)_x\right)\right]\right) d\Omega - \int_{\Gamma} \Psi \frac{1}{\mu}\frac{\partial \vec{A}}{\partial \vec{n}} d\Gamma = 0 \quad (40)$$

After an integration by parts and applying the condition of NEUMANN, we obtain the relation (41):

$$\begin{aligned}&\iint_{\Omega}\frac{1}{\mu}\left(\left(\frac{\partial\Psi}{\partial x}\frac{\partial A}{\partial x}\right)+\left(\frac{\partial\Psi}{\partial y}\frac{\partial A}{\partial y}\right)\right)d\Omega\\&+\iint_{\Omega}\Psi\cdot\left(-J_s+\sigma\frac{\partial A}{\partial t}\right)d\Omega\\&+\iint_{\Omega}\frac{1}{\mu}\left(-\frac{\partial\Psi}{\partial x}\left((B_r)_y\right)+\frac{\partial\Psi}{\partial y}\left((B_r)_x\right)\right)d\Omega=0\end{aligned} \tag{41}$$

The integration on an element and the approximation of the unknown function gives us the relation (42)

$$\begin{aligned}&\iint_{\Omega^e}\frac{1}{\mu}\left(\left(\frac{\partial\Psi^e}{\partial x}\frac{\partial\alpha^e}{\partial x}\right)+\left(\frac{\partial\Psi^e}{\partial y}\frac{\partial\alpha^e}{\partial y}\right)\right)A^e d\Omega\\&+\iint_{\Omega^e}\Psi^e\cdot\left(-J_s+\sigma\alpha^e\frac{\partial A^e}{\partial t}\right)d\Omega\\&+\iint_{\Omega^e}\frac{1}{\mu}\left(-\frac{\partial\Psi^e}{\partial x}\left((B_r)_y\right)+\frac{\partial\Psi^e}{\partial y}\left((B_r)_x\right)\right)d\Omega=0\end{aligned} \tag{42}$$

The choice of the weighting function is multiple and leads to several methods, among others, the Galerkine method of choosing as a weighting function Ψ_i^e the interpolation function α_i^e. Applying this method to equation (42) with integration on an element gives us

$$\begin{aligned}&\iint_{\Omega^e}\frac{1}{\mu}\left(\left(\frac{\partial\alpha^e}{\partial x}\frac{\partial\alpha^e}{\partial x}\right)+\left(\frac{\partial\alpha^e}{\partial y}\frac{\partial\alpha^e}{\partial y}\right)\right)A^e d\Omega\\&+\iint_{\Omega^e}\alpha^e\cdot\left(-J_s+\sigma\alpha^e\frac{\partial A^e}{\partial t}\right)d\Omega\\&+\iint_{\Omega^e}\frac{1}{\mu}\left(-\frac{\partial\alpha^e}{\partial x}\left((B_r)_y\right)+\frac{\partial\alpha^e}{\partial y}\left((B_r)_x\right)\right)d\Omega=0\end{aligned} \tag{43}$$

In matrix form the expression is written with relation (44):

$$[S]^e\ [A]^e - [P]^e + \sigma[T]^e\frac{\partial[A]^e}{\partial t} - [K]^e\ = 0 \tag{44}$$

Where:

$$S_{ij}^e=\int_{\Omega_e}\frac{1}{\mu}\left(\frac{\partial\alpha_i^e}{\partial x}\frac{\partial\alpha_j^e}{\partial x}+\frac{\partial\alpha_i^e}{\partial y}\frac{\partial\alpha_j^e}{\partial y}\right)d\Omega \tag{45}$$

$$P_i^e=\iint_{\Omega^e}\alpha_i^e J_s d\Omega \tag{46}$$

$$T_{ij}^e=\iint_{\Omega^e}\sigma\alpha_i^e\alpha_j^e d\Omega \tag{47}$$

$$K_i^e=\iint_{\Omega^e}\frac{1}{\mu}\left(-\frac{\partial\alpha_i^e}{\partial x}\left(B_{ry}\right)+\frac{\partial\alpha_i^e}{\partial y}\left(B_{rx}\right)\right)d\Omega \tag{48}$$

$$[S][A]+\sigma[T]\frac{\partial[A]}{\partial t}=[F] \tag{49}$$

The FEMM4.2 Software[7]: The FEMM software is a suite of programs for solving electromagnetic problems at low frequencies in dimension 2 in a domain (symmetrical or asymmetrical). It deals with magnetic, electrostatic, heat propagation or current flow problems. We recall that we only deal with magnetic problems.

The FEMM software is subdivided mainly into three parts:

Interactive shell: This program is a Multiple Document interface preprocessing and post-processing for the several types of problems solved by FEMM (This program is a multi-document interface (MDI) application that preprocesses and post processes several types of problems solved by FEMM.):

Pre-processor or pre-treatment: It contains a grid as an interface to expose the geometry of the problem to be solved, to define the reference and the scale. It gives the possibility to define the physical properties of the material and the boundary conditions of the considered domain. Autocad DXF folders created can be imported to allow analysis of existing geometric shapes.

The Postprocessor or Post-processing: Here the solutions are displayed in the shape of the contour defined in the post-processing. The program also allows the user to inspect the field at a given point, to evaluate several different integrals and to integrate several entities of specific quantities along the contours programmed by the user.

The triangle.exe: Triangle.exe software meshes the region of the solution into a large number of triangles (elements), which is a vital part of the finite element process. It realizes the discretization of the geometry defined in small elementary triangle: it is the mesh.

Solvers: The following solvers are software programs that solve different problems: fkern.exe for magnetism; belasolv.exe for electrostatic; hsolv.exe for problems with heat flow; and the csolv.exe for power flow problems.

Each solver takes a set of data that describes the problem and solves the appropriate partial differential equations to obtain desired values anywhere in the solution domain.

The Lua Script: Script Lua is a software integrated into the interactive shell. It makes it possible to build and analyze a geometry, to evaluate the treatment after the result and to make various simplifications. Lua is an extended programming language, designed for general programming procedures with ease of data description.

The Lua script is a part of a program directly interpreted by FEMM, containing functions specific to the FEMM software.

Applications: A Synchronous Machine modelling (ASM)[8,9]

In this part, we will model an asynchronous machine and a permanent magnet machine in healthy operation then with default. Table-1 gives us the characteristics of the asynchronous machine.

Table-1: characteristics of the asynchronous machine.

Characteristics of construction	Value Allocated	Unit
Pair of poles	2	-
Stator slots	48	-
Spiers by notches	2*50	-
Winding connection	Star	-
Stator outer radius	84	Mm
Stator interior radius	69.5	Mm
Bore radius	55	Mm
Rotor outer radius	54.6	Mm
Radius of the tree	16.5	Mm
Gap width	0.4	Mm
Effective length	160	Mm
Resistance to the stato	2.2	Ω
Stator inductance	108	mH
Rotor resistance	0.4	Ω
Phase voltage	220	V
Power frequency	50	Hz
Synchronous speed	1500	R.p.m
Slip	4.1	%
Phase current	12	A
Nominal torque	37	N.m
Power	5.5	KW

At the preprocessor stage of FEMM, the geometry of the healthy machine was represented using the properties of nodes, segments and arcs in dimension 2 (Figure-2): for more precision we used the Lua script.

In this case we defined four materials including M19-steel, copper (Copper), aluminum and air in the properties of materials and with the help of the right click and the spacebar on assigns the properties to the various regions. The stator and the rotor consist of plane-rolled steel sheet with a filling factor of 98%, the rotor notches contain aluminum windings and the stator windings contain copper windings. A homogeneous Dirichlet condition is applied.

The windings are fed by a three-phase network A, B, C at 50 Hz passing a current of 12A per phase defined in the circuit property. At each notch, the phase which feeds the windings is specified and the direction of progression of the current is specified with the positive or negative sign for the round trip. All windings of one phase are in series. The mesh of the structured model in 31729 nodes and 62714 elements is presented in Figure-3.

By adopting the same characteristics as before, we realize short circuits between two neighboring phases. The mesh of the model is structured in 32806 nodes and 64868 elements. The result of the mesh is presented in Figure-3: a) healthy asynchronous machine, b) asynchronous machine with defect.

Analysis and discussions

After meshing the models will be analyzed by FEMM fkern solver that will treat each element by solving the equation (49) in order to find the potential of the resulting vector A. Then he deduces the field and the magnetic induction and all the other parameters that the post-processor can display. Once completed the post processor can be loaded for data exploitation. The results of the post processor that we exploit are: Iso Potential vector lines and magnetic induction vector, magnetic flux density, curve plots and integral calculations. The flux lines and the induction vector are shown in Figure-4: a) for the healthy asynchronous machine, b) for the asynchronous machine with fault.

The flux density is shown in Figure-5: a) for the healthy asynchronous machine, b) for the asynchronous machine with fault.

The curves of the induction and the magnetic field are shown in Figure-6: a_1) and a_2) for the healthy asynchronous machine, b_1) and b_2) for the asynchronous machine with fault.

The places where the flux lines are closer together, the density of flux is high which determines the value of the vector of the magnetic induction which reigns in these zones. Field lines produced by each pole and phase are observed.

Note that the architecture of the flow lines in the event of a fault is different from the first case. Thus the flux lines are generated by the windings of healthy phases while for the turns in default there is no flux generated, they are the seat of interference of flux lines from two neighboring phases in default.

Figure-6 gives us a general idea about the distribution of induction in the machine. Induction values are locally higher in the gap than in other parts of the machine. It can be noticed that the magnetic induction is a periodic function which extends between a maximum of 2.75 T and a minimum of 0.5 T.

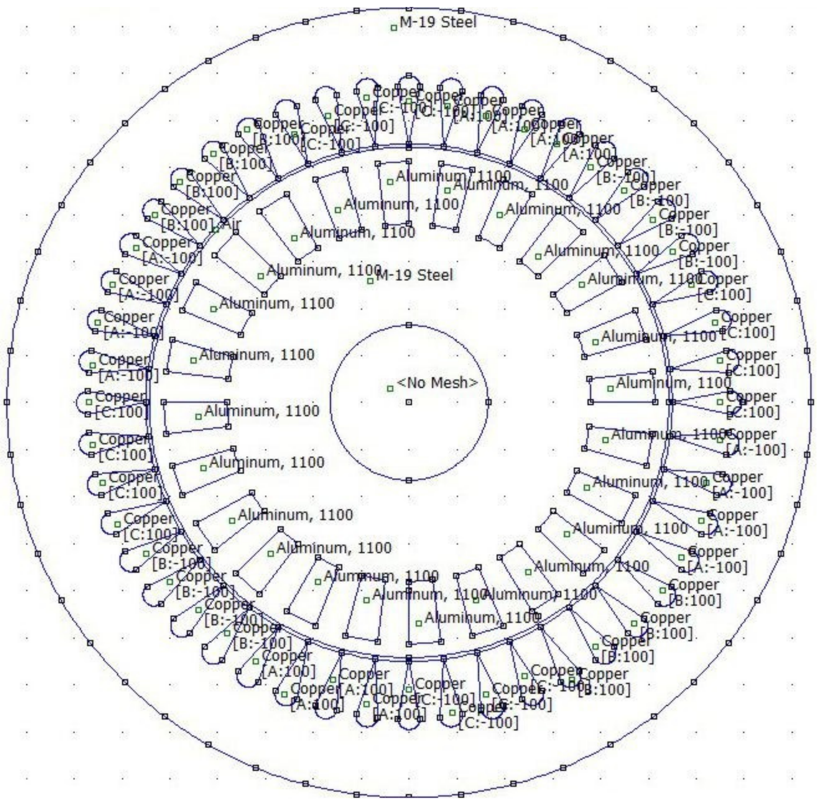

Figure-2: Healthy ASM model, figure obtained from FEMM 4.2 simulation Software.

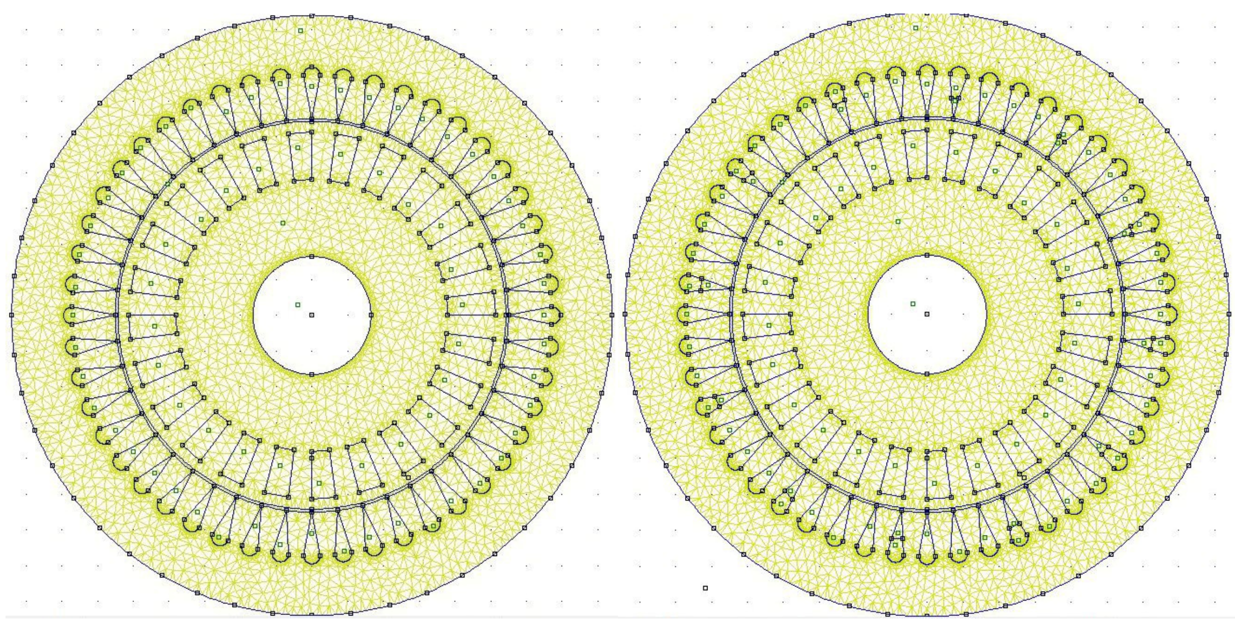

a) Healthy ASM b) ASM in default

Figure-3: Mesh model, figure obtained from FEMM 4.2 simulation Software.

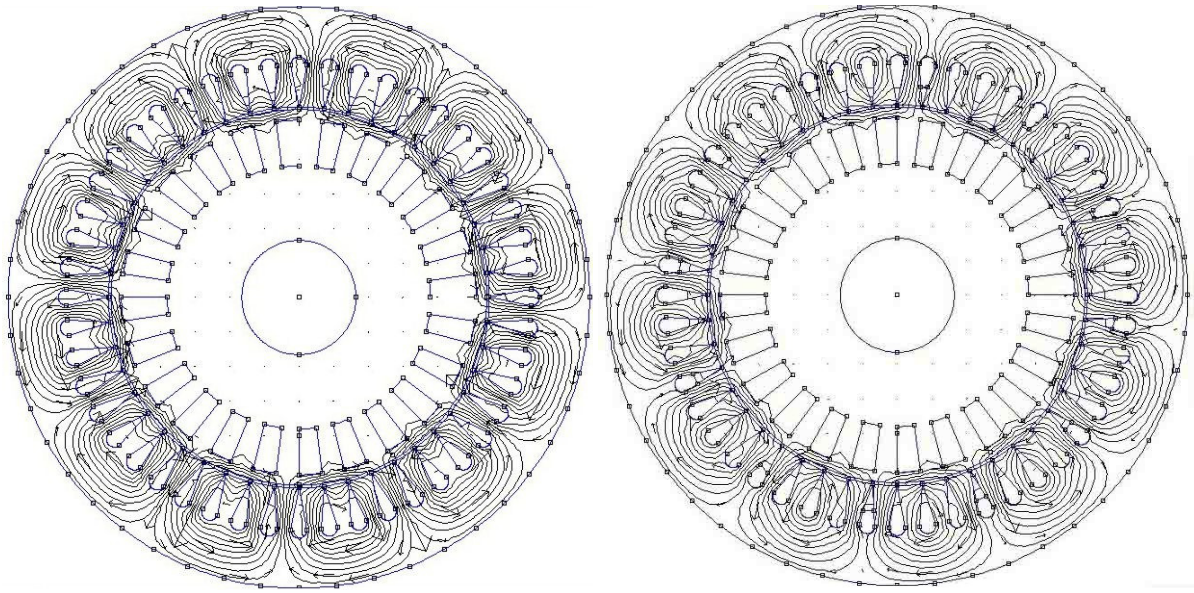

a) Healthy ASM b) ASM in default

Figure-4: Flux lines and induction vector; figure obtained from FEMM 4.2 simulation Software.

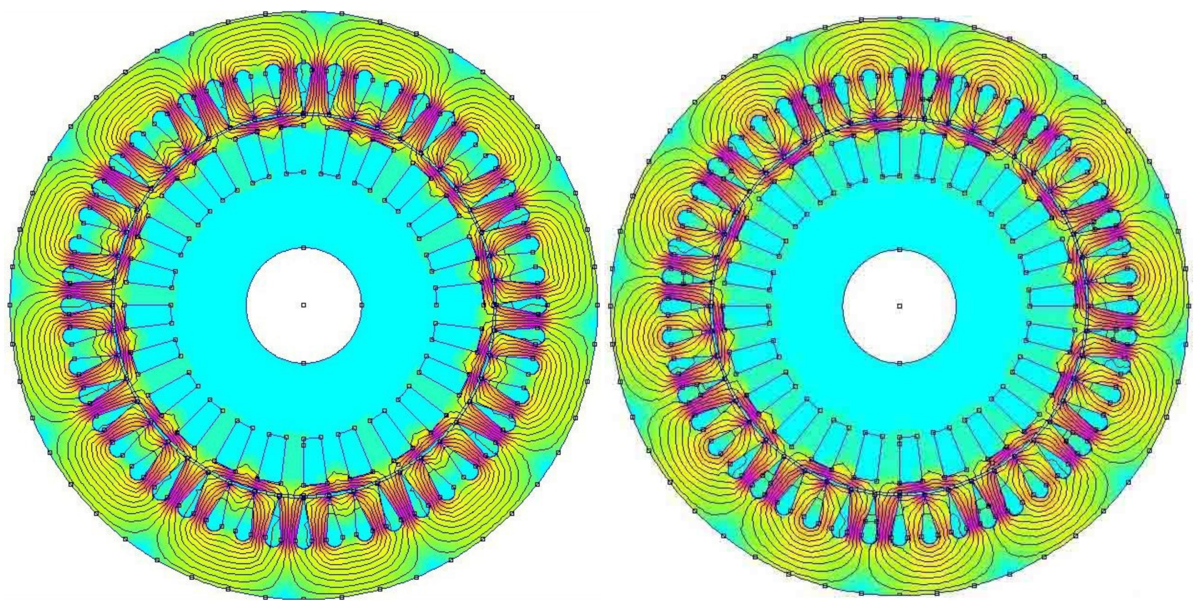

a) Healthy ASM b) ASM in default

Figure-5: Representation of the flux density, figure obtained from FEMM 4.2 simulation Software.

We can see that the value of the magnetic field in the gap and the field We can see that the value of the magnetic field in the air gap and the field created by the windings are proportional with a ratio of proportionality that equals the value of the permeability of the medium. Indeed the thickness of the air gap is very small compared to the length of the field lines, these lines through it without much loss. Since the stator is made of steel and the air gap contains air, we can write that:
$B_{steel} = B_{air}$ which implies that the product of μ steel, μ0 and H_{steel} is equivalent to the product of μ_0 and H_0 so the product μ steel and H_{steel} equals H_0[10]

Thus the magnetic excitation in the gap H_0 is the product of the permeability of steel with its excitation which is verified. It may be noted that the impact of the defect has resulted in a partial reduction of the induction in the gap. Similarly, the value of the magnetic field is partially reduced in the gap.

It is proposed to evaluate the intrinsic inductances of the magnetic circuit in the two operating cases (faultless and with default) and the results of the applications are presented in Table-2:

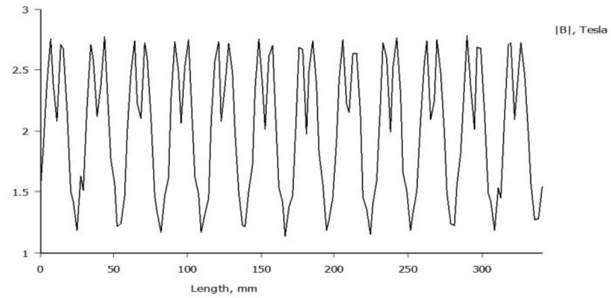

a_1) Healthy ASM

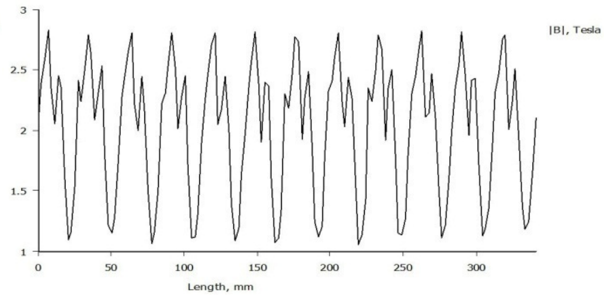

b_1) ASM in default

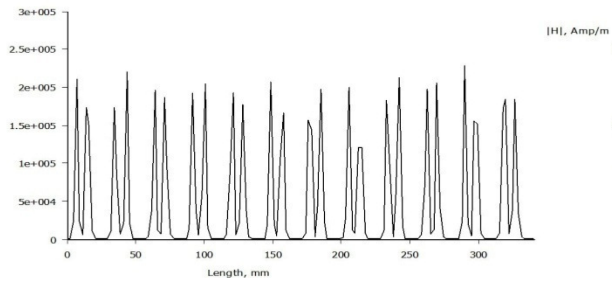

a_2) Healthy ASM

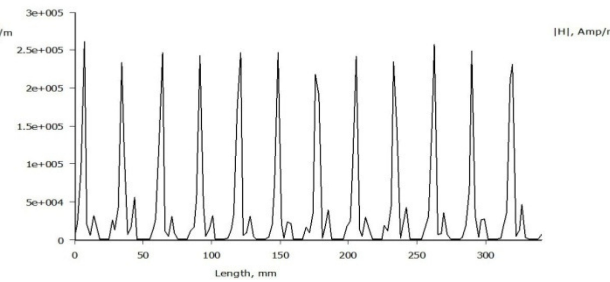

b_2) ASM in default

Figure-6: Magnetic induction and magnetic field in the air gap, figure obtainedfrom FEMM 4.2 simulation Software.

Table-2: Inductance Values.

Phases	Healthy Case Inductance (mH)	Inductance Default Case (mH)
A	254.210	241.959
B	254.340	242.155
C	254.610	241.760

Note that the value of the intrinsic inductance of the circuits has decreased. But we know that when a current flows through a conductor a swirling flux is established around it, which explains the value of the inductance in the wire. And if the faulty windings do not generate flux, this explains the decrease in the inductance and the density of the resulting flux in the gap.

Conclusion

The continuity of operation and the elimination of downtime in industrial installations is a factor that favors the development of the study of the art of state monitoring of electrical machines. This brings the world of researchers and engineers to the development of new diagnostic methods, one of which is electromagnetic monitoring.

The popularization and the development of the computer tool are among the reasons which projected the numerical methods in front of the modeling.

One of the methods used for this purpose is the finite element method which makes it possible to integrate all the phenomena inherent to the operation of machines such as saturation and movement. The FEMM 4.2 software based on the finite element method makes it possible to integrate the electromagnetic parameters during a modeling. In this paper, he allowed us to model an asynchronous machine by analyzing the propagation of flux lines and the density of the magnetic field. Also we were able to evaluate the intrinsic inductances of the circuits during a healthy operation then and with short-circuit failure between turns for a synchronous machine with permanent magnet where we have highlighted the reduction of the residual induction of the magnets due to a negative excitement.

Thus we obtained precise models of the behavior of the field lines and the magnetic state of the machine according to these defects.

References

1. Nedjar Boumedyen (2011). Modélisation basée sur la méthode des réseaux de perméances en vue de l'optimisation de machines synchrones à simple et à double excitations. Thèse de doctorat à l'Ecole Normale Supérieure de CACHAN.
2. Burnett David (1987). Finite Element Analysis form concepts to applications. Addison-Wesley Pub. Co., US, 1-844. ISBN: 97020110064.
3. Claude Chevassu (2012). Cours et Problème sur les machines électriques. 195-244.
4. Claude Divoux (1999). Milieux ferro ou ferrimagnétiques. 1-5.
5. Mohamed O. (2011). Elaboration d'un modèle d'étude en régime dynamique d'une machine à aimants permanents.

Mémoire de Magister à l'Université Mouloud Mammeri de TIZI-OUZOU.

6. Binns K.J., Trowbridge C.W. and Lawrenson P.J. (1992). The analytical and numerical solution of electric and magnetic field. Wiley-Blackwell, US, 1-486, ISBN-10: 0471924601, ISBN-13: 978-0471924609.

7. David Meeker (2006). Manuel d'utilisation de FEMM 4.2. 1-10.

8. Farooq Jawad Ahmed (2008). Etude du problème inverse en électromagnétisme en vue de la localisation des défauts de désaimantation dans les actionneurs à aimants permanents. Thèse de doctorat à l'Université de technologie de Belfort-Montbéliard.

9. Vaseghi Babak (2009). Contribution à l'étude des machines électriques en présence de défaut entre spires : Modélisation et réduction du courant de défaut. Thèse de doctorat à l'Institut National Polytechnique de Lorraine.

10. Gaëtan D. (2004). Modélisation et diagnostic de la machine asynchrone en présence de défaillance. Thèse de doctorat à l'Université Henri Poincarré, Nancy I.